PAPER

Single-molecule surface-enhanced Raman spectroscopy with nanowatt excitation

Brendan L. Darby, Pablo G. Etchegoin† and Eric C. Le Ru*

We demonstrate the possibility of single molecule (SM) detection *via* surface-enhanced Raman spectroscopy (SERS) in two seemingly challenging and unexpected cases: first with ultra-low excitation powers of the order of nanowatts and second in as-synthesized and not deliberately-aggregated silver colloid solution. The experiments are carried out using the bi-analyte method on a methylated form of Rhodamine 6G and one of its isotopologues excited at 514 nm close to the electronic resonance. This study spectacularly highlights the fact that SM-SERS detection is much more common and easier to achieve than typically thought, in particular in the case of resonance Raman excitation. As a result, SM-SERS detection in such cases should not be viewed as an indication of good SERS substrate performance as sometimes implicitly assumed.

1 Introduction

Surface-enhanced Raman spectroscopy (SERS)[1,2] is a technique exploiting the large electromagnetic field enhancements that can be obtained on the surface of metallic nanostructures to boost the Raman signal of adsorbed molecules by several orders of magnitude. The SERS enhancement factors (EFs) at specific points on the surface (so-called hot-spots) can be very large, of the order of 10^9–10^{10} for a given molecule under the best conditions,[3,4] and the power of SERS as an analytical tool is perhaps most dramatically demonstrated through its ability to observe Raman spectra from individual molecules.[5–10] At this level, SERS can even detect natural isotopic substitutions,[11] *i.e.* it is sensitive to a change of one unit mass in one atom of one molecule. Single-molecule SERS can therefore be exploited to study surface properties with exquisite detail, including for example the homogeneous and inhomogeneous broadening of Raman peaks,[12,13] resonance Raman excitation profiles,[14] and electrochemical properties[15,16] of single molecules. The conditions under which SM-SERS detection is obtained remain however difficult to control notably because of the extreme variation of enhancement factors on the surface (which results in the concept of hot-spots)[17,18] and the extreme sensitivity of those hot-spots to geometric parameters.[19] In fact, *average* SERS enhancement factors are much more modest, typically ranging from 10^4 to 10^6.[20] There is an intense research effort to fabricate

SERS substrate with improved reproducibility on the one hand[21–23] and improved SERS performance on the other. The latter aspect is fraught with problems, as there is no accepted standard of assessing it rigorously and quantitatively, and many estimates of SERS enhancement factors in the literature are not adequately justified.[24]

As an alternative, some studies have emphasized the capability of a given substrate for SM-SERS detection as a demonstration of the "exceptional" performance of a SERS substrate.[25–27] We here demonstrate that this is a misguided approach by highlighting how easy it can be to measure SERS from a single-molecule in the case of resonant excitation, such as Rhodamine 6G at 514 or 532 nm excitation. Specifically, we use the bi-analyte SERS technique[10,28] to evidence single-molecule detection at ultra-low excitation powers of 5 nW, *i.e.* a million times smaller than used in typical SERS experiments. To strengthen further our point, we also show that one of the simplest SERS substrates, as-synthesized silver colloid solution, is also capable of SM detection. These results clearly demonstrate "how easy" single molecule SERS detection can be for resonant excitation and emphasizes the fact that SM detection of resonant dyes cannot by itself be considered as a proxy for good SERS substrate performance.

2 Experimental

Synthesis

All reagents were purchased from Sigma-Aldrich and used as received. Lee & Meisel colloids (for the dried substrate experiments) were synthesized following ref. 29. For the experiments in solution, we instead use hydroxalamine-reduced colloids, synthesized according to ref. 30, which offer a narrower size distribution. Rhodamine 6M, or 3,6-bis(ethylamino)-9-[2-(methoxycarbonyl)phenyl]

The MacDiarmid Institute for Advanced Materials and Nanotechnology,
School of Chemical and Physical Sciences, Victoria University of Wellington,
PO Box 600, Wellington 6140, New Zealand. E-mail: eric.leru@vuw.ac.nz
† Sadly, Pablo Etchegoin passed away on 29 April 2013, aged 48, shortly after starting some of the experiments presented in this work. http://www.royalsociety.org.nz/organisation/academy/fellowship/obituaries/pablo-gabriel-etchegoin/

This journal is © the Owner Societies 2014

Phys. Chem. Chem. Phys., 2014, **16**, 23895–23899 | 23895

xanthylium, denoted R6M and its deuterated version, 3,6-bis-(ethylamino)-9-[2-(methoxycarbonyl)-d4-phenyl] xanthylium, denoted d4-R6M were synthesized and characterized as previously reported.[31]

Sample preparation

For the nanowatt excitation measurements, the Lee & Meisel Ag colloids were pre-aggregated for one hour in 10 mM KCl[32] and a mixture of R6M + d4-R6M was then added to a final concentration of 5 nM each. A drop of the solution was then left to dry on a silicon wafer until fully dried. Measurements were carried out in the center of the drop where the cluster concentration is not too high. For immersion measurements, solutions were prepared in two steps: First, the hydroxylamine-reduced Ag colloids were mixed in equal volumes with 1 mM KCl, which does not affect colloidal aggregation but facilitates rhodamine adsorption.[33] For the reference samples, a 20 nM solution of either R6M or d4-R6M was mixed in equal volumes (half–half dilution[34]) with the starting colloid + KCl solution yielding a final dye concentration of 10 nM. For bi-analyte samples, the same procedure was performed but by mixing equal volumes of a solution containing 4 nM of both dyes (R6M and d4-R6M) with the colloid + KCl solution, yielding a final concentration of 2 nM for each dye. The as-synthesized nanoparticle concentration is of the order of 1 nM (estimated from UV/Vis extinction and Mie theory assuming 15 nm radius Ag sphere in water[2]), so we can estimate that there are on average 8 dyes of each type on each nanoparticle for the bi-analyte experiment (since the colloids have been diluted 4 times in the final solution).

Raman set-up

All Raman and SERS experiments were carried out with a Jobin-Yvon Labram HR spectrometer, equipped with a liquid nitrogen cooled CCD detector, in the back-scattering configuration through a microscope objective. The samples were excited with a 514 nm Argon-ion laser and filters were used to reduce the power as needed. Laser powers were measured at the sample and are specified in the Results section along with integration times. A ×100 Olympus air objective NA 0.9 was used for dried substrates measurements, and a ×100 Olympus water immersion NA 1.0 for solutions. Raman maps were acquired using a motorized stage by scanning a 45 μm × 45 μm area with 1.5 μm steps (total of 900 spectra).

Bi-analyte experiments analysis

All SERS spectra obtained in the bi-anlayte experiments are fitted over the region of interest 560–650 cm^{-1} (or 1280–1400 cm^{-1} for Fig. 2(e)) as a linear combination of the reference spectra of each of the dye and a linear background, explicitly: $I((\bar{\nu})) = \alpha I_{R6M}((\bar{\nu})) + \beta I_{d4-R6M}((\bar{\nu})) + \gamma \bar{\nu} + \delta$. Such fits are carried out using a linear least-square fitting algorithm, which is both very efficient and stable. From the coefficients α and β, possible SM-SERS events can be easily identified and further investigated on a case-by-case basis.

SERS EF estimates

The SERS cross-section for each SM event is determined by normalization to a Raman cross-section standard as explained in ref. 3. For dried substrate measurements, nitrogen gas, as measured in air under ambient conditions with a power of 5 mW and integration time of 1800 s, was used as a reference Raman standard with $d\sigma/d\Omega = 4.3 \times 10^{-31}$ cm^2 sr^{-1} at 514 nm.[2,35] The effective scattering volume was estimated to be 5 μm^3 and the (Gaussian) beam waist w_0 of the order of 0.45 μm. For measurements in solution, 2-bromo-2-methylpropane is here used as the absolute Raman cross-section standard with $d\sigma/d\Omega = 1.3 \times 10^{-29}$ cm^2 sr^{-1} at 514 nm.[3] The effective scattering volume was estimated to be 10 μm^3 and the beam waist w_0 of the order of 0.6 μm. The single-molecule enhancement factor (SMEF) is then deduced by normalizing the SERS cross-section to the bare cross-section of the 612 cm^{-1} mode of Rhodamine 6G at 514 nm: $d\sigma/d\Omega = 2.3 \times 10^{-24}$ cm^2 sr^{-1} as measured in ref. 36 and 37.

TEM images

Samples for Transmission Electron Microscopy (TEM) imaging were prepared by centrifuging 1 mL of hydroxylamine-reduced Ag colloids (8000 rpm for 20 min at 29 °C) and redispersing them in 500 μL of milli-Q water. 7 μL of the redispersed colloids were then deposited on carbon-coated 400 square mesh copper grids. TEM grids were left to dry in a covered container for ∼6 hours. TEM images were collected with a JEOL JEM-1400PLUS instrument operating at 120 kV.

3 Results and discussion

Fig. 1(a) shows representative spectra obtained from a bi-analyte SERS experiment at an ultra-low excitation power, down to 5 nW. The experiment is carried out on Lee & Meisel Ag colloids pre-aggregated in 10 mM KCl[32] and with 5 nM concentration of each dye, and then dried on a silicon substrate. This results in colloid aggregates with hot-spots at the gaps[38] suitable for SM-SERS detection.[10] We use an excitation wavelength of 514 nm, which is close to the maximum of electronic absorption of both dyes at 526 nm and therefore expected to result in resonance Raman scattering. The SERS spectra of the two bi-analyte partners can be clearly distinguished in the region 560–650 cm^{-1} as seen in the reference spectra shown in Fig. 1. SERS spectra for the bi-analyte experiment are acquired at points on the substrate by 2D-scanning in 1.5 μm step increments. Representative examples of mixed and pure events are shown in Fig. 1, and the derived single-molecule enhancement factor (SMEF) are specified for each SM-event.

Although it may appear surprising that a Raman spectrum from a single molecule can be measured with such a low excitation power, it can in fact simply be explained from the following arguments. The resonance Raman cross-section in such cases is of the order of 10^{-24} cm^2 sr^{-1} (ref. 36, 37, 39 and 40) and modern Raman micro-spectrometers can detect a Raman peak equivalent to a cross-section of 10^{-21} cm^2 sr^{-1} under standard conditions with a high NA objective, ∼5 mW excitation power, and ∼0.1 s integration time[41] (to fix ideas, this corresponds to around 1000 Raman photons collected by the objective for a given Raman mode). A single-molecule EF of only 10^3 (which is present in the
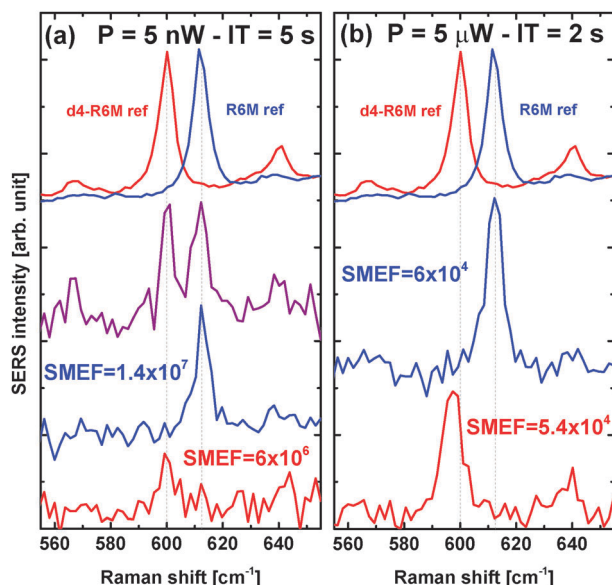
23896 | *Phys. Chem. Chem. Phys.*, 2014, **16**, 23895–23899

This journal is © the Owner Societies 2014

Fig. 1 Ultra-low power single-molecule SERS, evidenced using the bi-analyte method[10] with R6M (a methylated version of Rhodamine 6G, blue lines) and one of its isotopologues (d4-R6M,[31] red lines) excited at 514 nm, *i.e.* in resonance Raman conditions. The experiment is carried out on a dried substrate of aggregated Ag Lee & Meisel colloids deposited on a silicon wafer. In the left panel (a), a laser power of 5 nW only is used, with an integration time of 5 s. We show from top to bottom (using offsets for clarity) reference SERS spectra of both dyes, a *mixed* (R6M + d4-R6M) event, a representative *single* R6M molecule event, and one of the smallest detectable single d4-R6M events. Single-molecule EF are indicated where relevant. The SM-SERS events with the largest intensities reveal a maximum SMEF for this substrate of the order of $\sim 5 \times 10^7$. This maximum EF cannot be observed at higher powers due to limitations imposed by the photostability of the probe. This is illustrated explicitly in the right panel (b) showing similar results obtained at 1000 times more laser power.

majority of SERS substrates) is therefore sufficient for single-molecule detection at resonance at such standard powers. The reduction in power is here compensated by the larger SERS EF, estimated to be of the order of $\sim 10^7$ and a longer integration time of 5 s. It is worth highlighting that this enhancement factor is still much smaller than the largest typically used ($\sim 10^9$–10^{10}) for SM detection of pre-resonant[3,4] or non-resonant[42] molecules. With such optimized EF, SM-SERS would therefore be possible at even lower power (*e.g.* picowatts). It is also interesting to note that the same experiment at 5 mW does not result in a significant increase in SERS intensity (far from one-million-fold) because of photobleaching effects (evidenced and discussed in detail in ref. 43). In fact, these effects are even observable at powers as low as 5 μW as shown in Fig. 1(b), where the maximum single-molecule EF observable for an integration time of 2 s is only of the order of 5×10^4, *i.e.* 200 times less than observed at 5 nW.

This highlights how easy SM-SERS can be on a SERS substrate with maximum SERS EFs of $\sim 10^7$, which are large but far from the largest achievable. The same arguments would indicate that observing SM-SERS with a poor SERS substrate (with maximum EFs as low as 10^3–10^4) is also possible at standard excitation powers (mW). We have indeed recently

demonstrated SM-SERS detection in colloidal solutions of single-nanoparticles (gold bipyramids),[44] as opposed to inter-acting particles with gap hot-spots. The single-molecule SERS EFs in these experiments were in the range 10^5–10^6 only,[44] but this was enough to observe SM-SERS in pre-resonant conditions (crystal violet excited at 633 nm). A similar conclusion was recently obtained on single triangular nano-pyramids fabricated by nanosphere lithograpy.[45] Both of those studies relied on specially designed pointy nanoparticles, where the SERS EF at the tip can be relatively large.[46]

Motivated by the nanowatt excitation results, we can go one step further and demonstrate SM-SERS detection in arguably one of the simplest SERS substrates: Ag colloidal solutions. Most of the early SM-SERS experiments[7–10] were carried out using colloid clusters, either formed in solution by addition of an aggregating agent (typically an electrolyte like KCl at ~ 10 mM concentration) or created on a surface by drying the colloidal solution. Those clusters exhibit very large SERS EFs, notably at the junction between the nanoparticles[38,47] and are therefore ideally suited for SM-SERS. In contrast, as-synthesized and not deliberately aggregated colloidal solutions are notorious for their poor SERS activity. This is because the majority of colloids are then single nanoparticles, with relatively low maximum and average SERS EF. For example, for a 30 nm diameter Ag sphere in water, Mie theory predicts[48] an average SERS EF (in the $|E|^4$-approximation[49]) of only 480 at 514 nm excitation, and a maximum EF of 2300. Even for non-spherical elongated Ag nano-particles modeled as a prolate spheroid of 35 nm long axis and 20 nm short axis (whose main LSP resonance peaks at 515 nm), the average and maximum EF (orientation-averaged to account for the fast rotation of the NPs[44]) only go up to 6×10^4 and 7×10^5, respectively.[46] In real Ag colloid solutions, it is possible that clusters or large elongated particles also contribute marginally to the SERS activity, but these must be rare as they are not visible in the UV/Vis extinction spectrum (Fig. 2(b)). To minimize such contributions we prepared hydroxylamine-reduced Ag colloid (following ref. 30) solution, which exhibit a much more narrow size and shape distribution of nanoparticles (notably with no large nanorods, see Fig. 2(a)), compared to the commonly used Lee & Meisel Ag colloids.[29] Solutions were prepared as described in Section 2. Reference samples contained 10 nM of R6M or d4-R6M while bi-analyte samples contained 2 nM of each dye. For the low dye concentration used here, no dye-induced aggregation is expected.[34] The resulting solution is therefore expected to be identical to the as-synthesized Ag colloid solution, with little (if any) nanoparticle clusters present. The UV/Vis extinction of the solution (shown in Fig. 2(b)) indeed exhibits a narrow peak at 405 nm with no long-wavelength tail. Moreover, the average SERS EF (taken as the analytical EF as defined in ref. 3) was measured for the spectra of the reference solutions (at 10 nM) and was found to be of the order of $\langle EF \rangle \sim 700$ only, which further indicates that clusters do not contribute much, if at all, to the SERS intensity.

By all measures, these non-deliberately aggregated Ag colloids therefore represent one of the poorest SERS substrates; yet their SM-detection capability were evidenced experimentally in

This journal is © the Owner Societies 2014

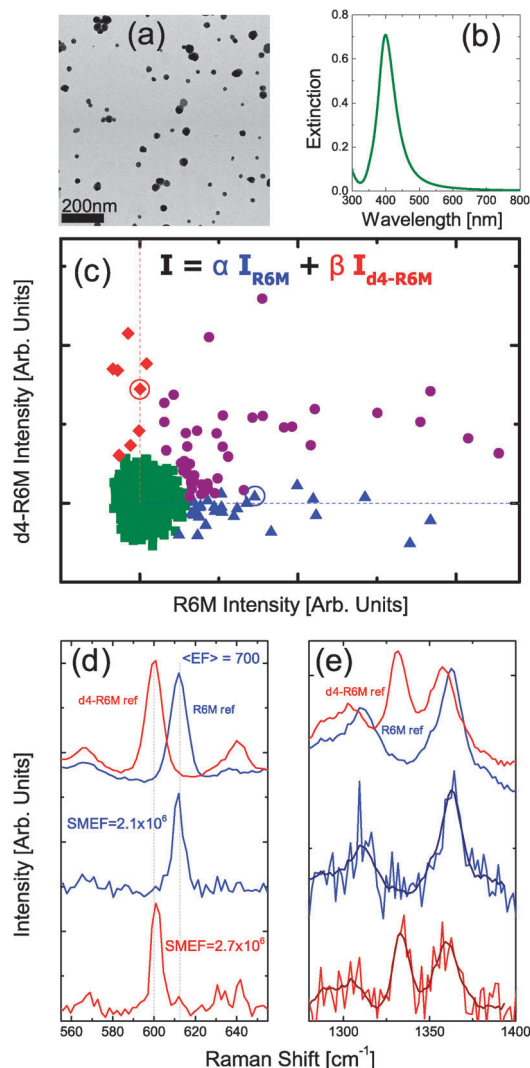*Phys. Chem. Chem. Phys.*, 2014, **16**, 23895–23899 | **23897**

Fig. 2 (a) TEM image of hydroxylamine-reduced Ag colloids. (b) Extinction spectrum of the sample used for the bi-analyte experiments (diluted 4 times for the UV/Vis measurement). (c) Statistical analysis of the bi-analyte SERS experiment (2 nM R6M + 2 nM d4-R6M) for as-synthesized colloids excited at 514 nm with a power of 0.2 mW and integration time of 0.4 s. 1000 individual spectra are measured and fitted (over the range $560-650$ cm^{-1}) to a weighted sum of the two reference spectra for each dye: $I = \alpha I_{R6M} + \beta I_{d4-R6M}$ (+ a linear background). The scatter plot for the 1000 values of α vs. β then enables to identify events below the noise (green), mixed events (purple), and likely SM events of either R6M (blue) or d4-R6M (red). Representative spectra marked by a circle in (c) are shown in (d) and (e) along with references in the two regions of interest where the Raman spectra differ. The result of the linear fits over the corresponding spectral range are also shown in (e).

bi-analyte experiments (Fig. 2(c–e)). Thanks to the Brownian motion, successive events relate to different nanoparticles, and by measuring 1000 consecutive spectra, the time series sampling is analogous to the 2D-mapping carried out earlier for a dry SERS substrate. Despite the poor performance of the substrate, bi-analyte experiments allowed us to identify SM-SERS events as shown in Fig. 2(d and e). Those events were associated with SMEF as low as $\sim10^6$, which would be consistent with elongated and/or faceted nanoparticles, although we cannot exclude that some also originate from rare nanoparticle clusters. In any case, this observation

demonstrates that SM-SERS detection can be evidenced in a seemingly poor SERS substrate.

4 Conclusion

In summary, this study clearly shows that most (if not all) SERS substrates should be capable of single-molecule detection in the easiest cases, such as for Rhodamine 6G excited at 514 or 532 nm. SM-SERS detection in such cases cannot be taken as an indication of good SERS substrate performance as often assumed. In fact, it is arguably more scientifically challenging to convincingly demonstrate single-molecule detection (for example using the bi-analyte method) than it is to achieve it. It should be noted however, that SM-SERS detection remains a challenge for small non-resonant molecules.[42] The conclusion of this work is quite clear: SM-detection is not in itself an indication of good SERS substrate performance, as sometimes implicitly assumed. Only carefully measured SERS EFs, which may in fact use SM-SERS as a tool, are convincing arguments of the SERS substrate capabilities. This study also reinforces that studying the maximum enhancement of the substrate requires the careful study of the photostability of the probe and its power dependence. The true maximum experimental enhancement (to compare with theory) might not otherwise be reliable if it is heavily influenced by photobleaching.

Acknowledgements

References

1 R. F. Aroca, Surface-Enhanced Vibrational Spectroscopy, John Wiley & Sons, Chichester, 2006.

2 E. C. Le Ru and P. G. Etchegoin, Principles of Surface Enhanced Raman Spectroscopy and Related Plasmonic Effects, Elsevier, Amsterdam, 2009.

3 E. C. Le Ru, E. Blackie, M. Meyer and P. G. Etchegoin, J. Phys. Chem. C, 2007, 111, 13794–13803.

4 S. L. Kleinman, E. Ringe, N. Valley, K. L. Wustholz, E. Phillips, K. A. Scheidt, G. C. Schatz and R. P. Van Duyne, J. Am. Chem. Soc., 2011, 133, 4115–4122.

5 E. C. Le Ru and P. G. Etchegoin, Annu. Rev. Phys. Chem., 2012, 63, 65.

6 N. P. W. Pieczonka and R. F. Aroca, Chem. Soc. Rev., 2008, 37, 946–954.

7 S. Nie and S. R. Emory, Science, 1997, 275, 1102–1106.

8 K. Kneipp, Y. Wang, H. Kneipp, L. T. Perelman, I. Itzkan, R. R. Dasari and M. S. Feld, Phys. Rev. Lett., 1997, 78, 1667–1670.

9 H. Xu, E. J. Bjerneld, M. Käll and L. Börjesson, Phys. Rev. Lett., 1999, 83, 4357–4360.

23898 | Phys. Chem. Chem. Phys., 2014, 16, 23895–23899

This journal is © the Owner Societies 2014

10 E. C. Le Ru, M. Meyer and P. G. Etchegoin, *J. Phys. Chem. B*, 2006, **110**, 1944–1948.

11 P. G. Etchegoin, E. C. Le Ru and M. Meyer, *J. Am. Chem. Soc.*, 2009, **131**, 2713–2716.

12 P. G. Etchegoin and E. C. Le Ru, *Anal. Chem.*, 2010, **82**, 2888–2892.

13 C. Artur, E. C. Le Ru and P. G. Etchegoin, *J. Phys. Chem. Lett.*, 2011, **2**, 3002–3005.

14 J. A. Dieringer, K. L. Wustholz, D. J. Masiello, J. P. Camden, S. L. Kleinman, G. C. Schatz and R. P. Van Duyne, *J. Am. Chem. Soc.*, 2009, **131**, 849–854.

15 E. Cortés, P. G. Etchegoin, E. C. Le Ru, A. Fainstein, M. E. Vela and R. C. Salvarezza, *J. Am. Chem. Soc.*, 2013, **135**, 2809–2815.

16 A. J. Wilson and K. A. Willets, *Nano Lett.*, 2014, **14**, 939–945.

17 E. C. Le Ru, P. G. Etchegoin and M. Meyer, *J. Chem. Phys.*, 2006, **125**, 204701.

18 S. M. Stranahan and K. A. Willets, *Nano Lett.*, 2010, **10**, 3777–3784.

19 J. P. Camden, J. A. Dieringer, Y. Wang, D. J. Masiello, L. D. Marks, G. C. Schatz and R. P. Van Duyne, *J. Am. Chem. Soc.*, 2008, **130**, 12616–12617.

20 E. C. Le Ru and P. G. Etchegoin, *MRS Bull.*, 2013, **38**, 631–640.

21 X. Zhang, J. Zhao, A. V. Whitney, J. W. Elam and R. P. Van Duyne, *J. Am. Chem. Soc.*, 2006, **128**, 10304–10309.

22 M. Roca and A. J. Haes, *J. Am. Chem. Soc.*, 2008, **130**, 14273–14279.

23 S. E. J. Bell and N. M. S. Sirimuthu, *Chem. Soc. Rev.*, 2008, **37**, 1012–1024.

24 M. J. Natan, *Faraday Discuss.*, 2006, **132**, 321–328.

25 H. Liu, L. Zhang, X. Lang, Y. Yamaguchi, H. Iwasaki, Y. Inouye, Q. Xue and M. Chen, *Sci. Rep.*, 2011, **1**, 112.

26 D. Wang, W. Zhu, M. D. Best, J. P. Camden and K. B. Crozier, *Nano Lett.*, 2013, **13**, 2194–2198.

27 P. P. Patra and G. V. P. Kumar, *J. Phys. Chem. Lett.*, 2013, **4**, 1167–1171.

28 P. G. Etchegoin, M. Meyer, E. Blackie and E. C. Le Ru, *Anal. Chem.*, 2007, **79**, 8411–8515.

29 P. C. Lee and D. Meisel, *J. Phys. Chem.*, 1982, **86**, 3391–3395.

30 N. Leopold and B. Lendl, *J. Phys. Chem. B*, 2003, **107**, 5723–5727.

31 E. Blackie, E. C. Le Ru, M. Meyer, M. Timmer, B. Burkett, P. Northcote and P. G. Etchegoin, *Phys. Chem. Chem. Phys.*, 2008, **10**, 4147–4153.

32 M. Meyer, E. C. Le Ru and P. G. Etchegoin, *J. Phys. Chem. B*, 2006, **110**, 6040–6047.

33 S. Kruszewski and M. Cyrankiewicz, *Acta Phys. Pol., A*, 2013, **123**, 965–969.

34 B. L. Darby and E. C. Le Ru, *J. Am. Chem. Soc.*, 2014, **136**, 10965–10973.

35 H. W. Schrötter and H. W. Klöckner, in *Raman scattering cross sections in gases and liquids*, ed. A. Weber, Springer, Berlin, 1979, pp. 123–166.

36 E. C. Le Ru, L. C. Schroeter and P. G. Etchegoin, *Anal. Chem.*, 2012, **84**, 5074.

37 B. Auguie, A. Reigue, E. C. Le Ru and P. G. Etchegoin, *Anal. Chem.*, 2012, **84**, 7938.

38 J. Jiang, K. Bosnick, M. Maillard and L. Brus, *J. Phys. Chem. B*, 2003, **107**, 9964–9972.

39 S. Shim, C. M. Stuart and R. A. Mathies, *ChemPhysChem*, 2008, **9**, 697–699.

40 A. Reigue, B. Auguie, P. G. Etchegoin and E. C. Le Ru, *J. Raman Spectrosc.*, 2013, **44**, 573–581.

41 P. G. Etchegoin and E. C. Le Ru, *Phys. Chem. Chem. Phys.*, 2008, **10**, 6079–6089.

42 E. J. Blackie, E. C. Le Ru and P. G. Etchegoin, *J. Am. Chem. Soc.*, 2009, **131**, 14466–14472.

43 P. G. Etchegoin, P. D. Lacharmoise and E. C. Le Ru, *Anal. Chem.*, 2009, **81**, 682–688.

44 E. C. Le Ru, J. Grand, I. Sow, W. R. C. Somerville, P. G. Etchegoin, M. Treguer-Delapierre, G. Charron, N. Felidj, G. Levi and J. Aubard, *Nano Lett.*, 2011, **11**, 5013.

45 A. B. Zrimsek, A.-I. Henry and R. P. Van Duyne, *J. Phys. Chem. Lett.*, 2013, **4**, 3206–3210.

46 R. Boyack and E. C. Le Ru, *Phys. Chem. Chem. Phys.*, 2009, **11**, 7398.

47 M. Futamata, Y. Maruyama and M. Ishikawa, *J. Mol. Struct.*, 2005, **735**, 75–84.

48 E. C. Le Ru and P. G. Etchegoin, *SERS and Plasmonics Codes (SPlaC)*, Matlab codes freely available from http://www.vuw.ac.nz/raman/book/codes.aspx.

49 E. C. Le Ru and P. G. Etchegoin, *Chem. Phys. Lett.*, 2006, **423**, 63–66.